Health, for maintenance of the UCSF Magnetic Resonance Laboratory. T.L.J. also acknowledges receipt of a Research Career Development Award (AM 00291) from the National Institutes of Health.

References and Notes

(1) M. Levitt and A. Warshel, *J. Am. Chem. Soc.*, **100**, 2607 (1978).
(2) M. D. Barkley and B. H. Zimm, *J. Chem. Phys.*, **70**, 2991 (1979).
(3) L. Kleven, I. M. Armitage, and D. M. Crothers, *Nucl. Acids Res.*, **6**, 1607 (1979).
(4) P. Davanloo, I. M. Armitage, and D. M. Crothers, *Biopolymers*, **18**, 663 (1979).
(5) K. Akasaka, A. Yamada, and H. Hatano, *Bull. Chem. Soc. Jpn.*, **50**, 2858 (1977).
(6) P. H. Bolton and T. L. James, *J. Am. Chem. Soc.*, in press.
(7) T. Early and D. R. Kearns, *Proc. Natl. Acad. Sci. U.S.A.*, submitted for publication.
(8) Ph. Wahl, P. Paoletti, and J.-B. LePecq, *Proc. Natl. Acad. Sci. U.S.A.*, **65**, 417 (1970).
(9) D. Genest and P. Wahl, *Biochim. Biophys. Acta*, **521**, 502 (1978).
(10) T. L. James, R. B. Matthews, and G. B. Matson, *Biopolymers*, **18**, 1763 (1979).
(11) V. A. Bloomfield, D. M. Crothers, and I. Tinoco, Jr., "Physical Chemistry of Nucleic Acids", Harper & Row, New York, 1974.
(12) H. B. Gray, Jr., and J. E. Hearst, *J. Mol. Biol.*, **35**, 111 (1968).
(13) C. P. Slichter, "Principles of Magnetic Resonance", Harper & Row, New York, 1963.
(14) (a) T. L. James, G. B. Matson, I. D. Kuntz, R. W. Fisher, and D. H. Buttlaire, *J. Mag. Reson.*, **28**, 417 (1977); (b) T. L. James, G. B. Matson, and I. D. Kuntz, Jr., *J. Am. Chem. Soc.*, **100**, 9490 (1978); (c) T. L. James and G. B. Matson, *J. Mag. Reson.*, **33**, 345 (1979).
(15) D. E. Woessner, *J. Chem. Phys.*, **36**, 1 (1962).
(16) D. Doddrell, V. Glushko, and A. Allerhand, *J. Chem. Phys.*, **56**, 3683 (1972).
(17) (a) W. E. Hull and B. D. Sykes, *J. Chem. Phys.*, **63**, 867 (1975); (b) *J. Mol. Biol.*, **98**, 121 (1975).
(18) M. Levitt, *Proc. Natl. Acad. Sci. U.S.A.*, **75**, 640 (1978).
(19) (a) S. Arnott, *Prog. Biophys. Mol. Biol.*, **21**, 265 (1970); (b) D. B. Davies, *Prog. Nucl. Mag. Reson. Spectrosc.*, **12**, 135 (1978).
(20) (a) M. Leng and G. Felsenfeld, *J. Mol. Biol.*, **15**, 455 (1966); (b) H. Eisenberg and G. Felsenfeld, *ibid.*, **30**, 17 (1967); (c) B. S. Stannard and G. Felsenfeld, *Biopolymers*, **14**, 299 (1975).

Nuclear Magnetic Shielding Density

Cynthia J. Jameson

Department of Chemistry, University of Illinois at Chicago Circle, Chicago, Illinois 60680

and A. D. Buckingham

Department of Theoretical Chemistry, Cambridge University, Lensfield Road, Cambridge CB2 1EW, England *(Received August 10, 1979)*

Publication costs assisted by the National Science Foundation

Molecular charge density maps have been widely used to characterize the bonding in a molecule, the facilitation or opposition of nuclear motion or the changes which occur in hydrogen bonding, and other intermolecular effects. In a similar fashion, nuclear magnetic shielding densities may be useful in providing a physical interpretation of gross differences between molecules in magnitudes of the nuclear shielding constants, their dependence on nuclear configuration, as well as more subtle differences or shifts which are observed in NMR. We explore the use of shielding density difference maps for the interpretation of chemical shifts which occur upon molecule formation. This concept appears to have great promise in providing a physical basis for interpretation of NMR shifts.

Introduction

Chemists generally discuss effects, contributions, and mechanisms in interpreting their experimental results. Thus, even as highly sophisticated programs are producing electronic energies, ground state electronic properties, and even anharmonic force constants for very light molecules, chemists continue to discuss electronic properties, such as NMR chemical shifts, in terms of relatively simple physical models such as lone pairs, ionic character, electronegativity, inductive effects, and steric hindrance. The difference between two very accurate numerical results of nuclear magnetic shielding for a given nucleus in two different molecules merely reproduces the magnitude of the observed chemical shift between them and provides little if any physical understanding. More than the magnitude of the chemical shifts between two molecules we would like to understand the observed solvent shifts, hydrogen bonding effects, isotope effects, and neighbor effects. These small effects can be reproduced only by very accurate calculations involving minute changes in the wave functions whose very complexity seriously handicaps any discussion based on a physical picture. As noted by Bader,[1] the difficulties in discussing the wave function itself are overcome to a large extent by employing directly the one-electron density distribution and density difference contours as the basis for the discussion of chemical concepts regarding the bonding in molecules, force constants, dipole moments, and other properties which are directly related to charge densities and forces acting on the nuclei.[2-4] Charge density maps have the advantage in that they do not increase in complexity as the form and the number of functions used in the wave function are changed. The fact that the one-electron density function predicts the distribution of electronic charge in real space permits a direct physical picture and a physical interpretation.[5]

We have proposed the use of property density maps for those molecular electronic properties which are not directly related to charge densities.[6] The integration of the property density function over all space gives the numerical value of the property in the same way that the integration of the charge density function over all space gives the number of electrons. From this analogy it should be obvious that the magnetic shielding density function, in particular, can be very useful in understanding changes in magnetic shielding upon molecule formation, interaction

0022-3654/79/2083-3366$01.00/0

TABLE I: ^1H and ^{19}F Nuclear Magnetic Shielding Constants for the HF Molecule, in ppm[a]

^1H				^{19}F				
σ_{xx}	σ_{zz}	$(\sigma_{xx}+\sigma_{yy}+\sigma_{zz})/3$	$\sigma_{zz}-(\sigma_{xx}+\sigma_{yy})/2$	σ_{xx}	σ_{zz}	$(\sigma_{xx}+\sigma_{yy}+\sigma_{zz})/3$	$\sigma_{zz}-(\sigma_{xx}+\sigma_{yy})/2$	ref
		28.45				413.85		26
		27.00				400.34		15
		26.281						15
24.2	43.5	30.6	19.3	376.2	482.8	411.7	106.6	11
18.852	44.096	27.267	25.244	379.236	481.939	413.470	102.703	12
19.7	44.1	27.8	24.4	377.7	481.9	412.4	104.3	13
30.08	44.41	34.86	14.33	383.37	478.45	415.07	95.08	14
		28.51 (±0.20)[a]	24[b]			410 (±6)[c]	108[b]	(expt)

[a] W. T. Raynes in "Nuclear Magnetic Resonance", Vol. 7, R. K. Harris, Ed., The Chemical Society, London, 1977. [b] F.H. De Leeuw and A. Dymanus, *J. Mol. Spectrosc.*, 48, 427 (1973). [c] D. K. Hinderman and C. D. Cornwell, *J. Chem. Phys.*, 48, 4148 (1968).

with another molecule, bond extension, etc. A recent review of the applications of the chemical shift indicates that the literature on substituent effects on chemical shifts is still dominated by the use of constructs such as inductive and resonance effects transmitted through chemical bonds or steric and electrical field effects transmitted through space, including ring currents.[7] With a mapping of the spatial distribution of the magnetic shielding density, it may be possible to have a physical basis for such discussions. It may even be possible with the help of shielding density maps to choose between alternative hypothetical physical interpretations of observed chemical shifts.

The general theory and the definition of the concept of property density functions for some electric and magnetic properties have been discussed previously.[6] It is shown that electric property densities can be expressed in terms of the charge density function whereas magnetic property densities can be expressed in terms of the current density. In the presence of a uniform static magnetic field, the current density may be expanded as a series in the field:

$$\mathbf{J}^{H} = \mathbf{J}^{H(0)} + \lambda\mathbf{J}^{H(1)} + \lambda^2\mathbf{J}^{H(2)} + \ldots$$

The magnetic shielding density function $\sigma^N(r)$ is defined as[6]

$$\sigma^N(\mathbf{r})\cdot\mathbf{H} = -(\mathbf{r}_N \times \mathbf{J}^H)/cr_N^3$$

where $\mathbf{J}^H$ is the current density to first order. $\mathbf{J}^{H(0)}$, the zeroth order current density, is zero for a diamagnetic molecule since the current density vanishes in the absence of a magnetic field. For a single electron $\mathbf{J}^{H(1)}$ is given by[8]

$$\mathbf{J}^{H(1)} = -\frac{e\hbar H}{im}(\psi^{(1)}\nabla\psi^{(0)} - \psi^{(0)}\nabla\psi^{(1)}) - \frac{e^2}{mc}\mathbf{A}_H\psi^{(0)}\psi^{(0)}$$

Thus, the magnetic shielding density function may be expressed as[6]

$$\sigma^N(\mathbf{r}) = \frac{e\hbar}{imcr_N^3}(\psi^{(1)}\mathbf{r}_N \times \nabla\psi^{(0)} - \psi^{(0)}\mathbf{r}_N \times \nabla\psi^{(1)}) + \frac{e^2}{mc^2r_N^3}\psi^{(0)}(\mathbf{r}_N\cdot\mathbf{r}I - \mathbf{r}_N\mathbf{r})\psi^{(0)}$$

in which $\psi^{(1)}$ is the first-order correction to the wave function in the presence of a static uniform magnetic field. The method of extending this definition to a many-electron system is discussed in the next section.

The current density itself has been of some interest.[9,10] The current density function has been shown to be gauge independent and its computation involves determination of the wave function which describes the electron when acted on by both the electrostatic potentials and the static magnetic field. Lipscomb gives contour maps of the current density in LiH, BH, AlH, N_2, and F_2, showing the contour maps of the modulus as well as the vector direction maps over the same region.[10] For example, in LiH, the currents are mainly diamagnetic around both Li and H but there is a small region in which paramagnetic circulation of current occurs. This paramagnetic current is found to be not large enough nor centered near enough to the Li nucleus to produce a large downfield chemical shift relative to the Li atom. With the aid of a current density map it would be possible to discuss both the molecular magnetic susceptibility and the chemical shielding of any nucleus N in the molecule. However, such discussions would require mentally taking the cross product of the current density vector at each point in the map with either $\mathbf{r}$ or $\mathbf{r}_N/\mathbf{r}_N^3$, respectively, for susceptibility and shielding. The shielding is more sensitive to nearby currents because of the r_N^{-3} factor in the integral, unless nearby currents are especially small. Current density maps are probably the appropriate density maps for discussing diamagnetic susceptibilities of molecules, since current densities $\mathbf{J}^H$ are gauge-origin independent whereas suceptibility density functions $(\mathbf{r} \times \mathbf{J}^H)/2c$ are intrinsically origin dependent. On the other hand, the magnetic shielding density function, $(\mathbf{r}_N \times \mathbf{J}^H)/cr_N^3$ is gauge independent just as $\mathbf{J}^H$ is. While current density maps have a more general applicability in that they may be used to discuss the shielding of *any* nucleus in the molecule, magnetic shielding density maps have a more direct physical relationship to magnetic shielding than current density maps do and are therefore the preferred physical basis for discussions of NMR chemical shifts.

The general theory, and the fine points of origin dependence, practical gauge dependence, uniqueness of off-diagonal components, and changes with bond extension are treated in detail in another paper.[6] Here we will illustrate the shielding density changes upon molecule formation. The molecule used as a test case is HF, for several reasons. There have been a large number of recent calculations of the components of the magnetic shielding of the nuclei in HF.[11-15] These are compared with experiment in Table I. As can be seen from Table I, the results of the calculations are becoming sufficiently accurate for a meaningful density function to be obtained. The H and F nuclei provide examples of a light and a heavy nucleus (from the point of view of NMR) so that the differing contributions of the diamagnetic and paramagnetic terms can be examined. In HF, the changes in the shieldings are not dominated by changes in the diamagnetic part alone. The magnetic shielding density functions for ^1H in HF, and for ^{19}F in HF, are calculated with the gauge origin on the F. The shielding density difference maps for molecule formation are illustrated with the ^1H shielding difference for HF relative to H atom and the ^{19}F

shielding difference for HF relative to F^- ion.

Method

Within the framework of the one-determinant approximation to the wave function, three fundamental approaches have been employed in computing nuclear magnetic shielding: coupled Hartree–Fock perturbation theory,[16-18] uncoupled Hartree–Fock perturbation theories at various levels of sophistication,[19-21] and variational techniques.[22-24] Caves and Karplus have given a comparative analysis of the coupled Hartree–Fock, the uncoupled Hartree–Fock, and Rebane's variational methods, and these procedures were shown to differ in the degree of electron correlation they account for.[25] In this respect, the coupled Hartree–Fock scheme is preferable.

Other difficulties arise in computing magnetic properties, since the vector potential appearing explicitly in the Hamiltonian is not uniquely determined but contains a gauge which can be chosen arbitrarily. Coupled Hartree–Fock procedures guarantee gauge invariance only when perturbed and unperturbed molecular orbitals are the exact solution of the Hartree–Fock problem,[26] which is not attained in actual calculations since finite basis sets are necessarily used. Translational invariance is achieved by expanding the molecular orbitals in a basis set of gauge dependent atomic orbitals (GIAOs).[27] However, while origin independent results are obtained in GIAO calculations, the fundamental physical requirement of current conservation is not met.[28] In addition, in expanding the basis set employed, the gauge factors in the GIAOs introduce numerical difficulties in evaluation of the necessary integrals, without substantial improvement of computed properties over the coupled Hartree–Fock calculation with the same size basis of gaugeless atomic orbitals.[27] The method used here is the coupled Hartree–Fock method with gaugeless Gaussian functions centered on the various atoms. The basis set used for HF (and F^- ion) is that given by Lie and Clementi which gives a total energy 0.0022 hartree away from the true Hartree–Fock solution.[29] It consists of 11 contracted functions from 14 primitive Gaussian functions centered on H and 31 contracted functions from 49 primitive Gaussian functions centered on F.

Since coupled Hartree–Fock perturbation theory is well known, we merely outline the equations used in the calculations. The one-electron Hamiltonian and the density matrix are written as a power series in the parameters H (magnetic field) and μ (nuclear magnetic moment):

$$h = f + \mathrm{G}(\mathbf{R})$$

$$f = f_0 + \lambda f^{(1)} + \lambda^2 f^{(2)} + \ldots$$

$$\mathbf{R} = \mathbf{R}_0 + \lambda \mathbf{R}^{(1)} + \lambda^2 \mathbf{R}^{(2)} + \ldots$$

In the case of magnetic properties[30]

$$f^{(1)} = a f^a + b f^b + \ldots$$

$$f^{(2)} = a^2 f^{a^2} + b^2 f^{b^2} + ab f^{ab} + \ldots$$

where

$$a = \alpha\mu$$

$$b = \alpha H$$

$$f^a = M_\mathrm{N}/r_\mathrm{N}^3$$

$$f^b = M_\mathrm{H}/2$$

$$f^{ab} = (\mathbf{r}_\mathrm{N}\cdot\mathbf{r} I - \mathbf{r}_\mathrm{N}\mathbf{r})/2r_\mathrm{N}^3$$

$$f^{b^2} = (\mathbf{r}^2 I - \mathbf{r}\mathbf{r})/8$$

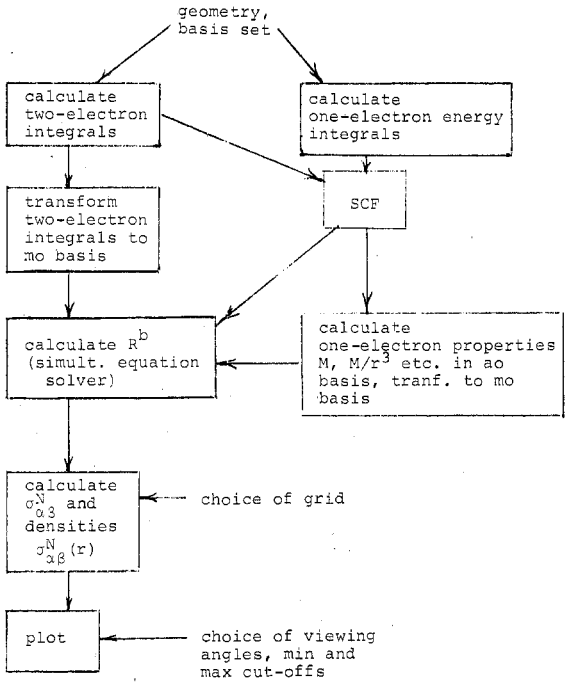

Figure 1. A brief flowchart of the calculations described in the text. Although calculations were carried out for various choices of gauge origin, only the results for gauge origin at F are shown in this paper.

Here $\alpha^2 = e^2/mc^2$ and M is the angular momentum operator. The subscript N indicates a vector defined with respect to the nucleus (N) of interest as the origin. The energy term of interest in the case of nuclear magnetic shielding is

$$\mu\cdot\sigma\cdot H = E^{ab} = 2(\mathrm{tr}\,[f^{ab}R^0 + f^a R^b]) = 2(\mathrm{tr}\,[f^{ab}R^0 + f^b R^a])$$

Within the coupled Hartree–Fock formulation given by McWeeny and Diercksen, the first-order density matrix $\mathbf{R}^b$ can be evaluated by solving the coupled linear simultaneous equations[17]

$$\mathbf{R}^b = \sum_r^{\mathrm{occ}} \sum_s^{\mathrm{unocc}} \frac{\Delta_{rs}{}^b}{\epsilon_r - \epsilon_s} \mathbf{C}_r \mathbf{C}_s^\dagger$$

where

$$\Delta_{rs}{}^b = \mathbf{C}_r^\dagger (f^b + \mathrm{G}(R^b))\mathbf{C}_s$$

In other words, the elements of the density matrix in the basis of unperturbed molecular orbitals $\psi_q{}^0$, $q = 1, \ldots, m$, are obtained by solving the simultaneous equations

$$R_{sq}{}^b = \{(r \times \nabla/2i)_{sq} \sum_{t=1}^{n} \sum_{u=n+1}^{m} R_{ut}{}^b[-(qt|us) + (qu|ts)]\}/(\epsilon_\mathrm{q} - \epsilon_\mathrm{s})$$

where $(qt|us)$ is the two-electron integral $\int \psi_q^*(1)\psi_t(1)\cdot\psi_u^*(2)\psi_s(2)/r_{12}\,\mathrm{d}\tau_1\,\mathrm{d}\tau_2$. The algorithm used is shown in Figure 1. The calculation of the integrals and the SCF calculation were carried out with the ATMOL3 package of programs.[31]

The shielding density function is a surface in four-dimensional space and its representation in its entirety on a two-dimensional chart is impossible. However, if we choose a particular plane in space, oriented in some fixed way relative to the molecular axes, then the shielding density values at the points on that plane can be represented as a three-dimensional surface. In this case the plane chosen was the $x = 0.0625$ au plane. A three-dimensional figure can be represented on a two-dimensional chart in several ways. One way is to plot contours connecting points of equal density. However, this requires

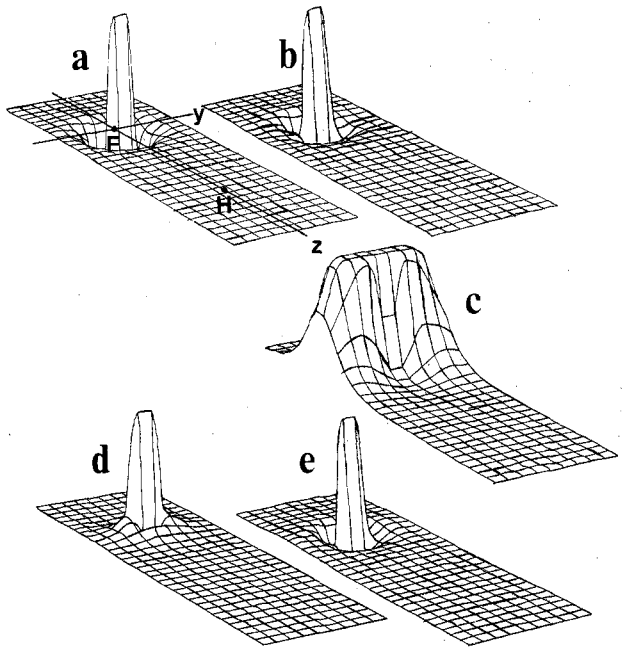

Figure 2. ^{19}F shielding density maps for the $x = 0.0625$ au plane of the HF molecule. The density maps shown are for the components (a) σ_{xx}, (b) σ_{yy}, (c) σ_{zz}, (d) $(\sigma_{xx} + \sigma_{yy} + \sigma_{zz})/3$, and (e) $\sigma_{zz} - (\sigma_{xx} + \sigma_{yy})/2$. The σ_{zz} mapping has been truncated in order to show the features on an expanded density scale.

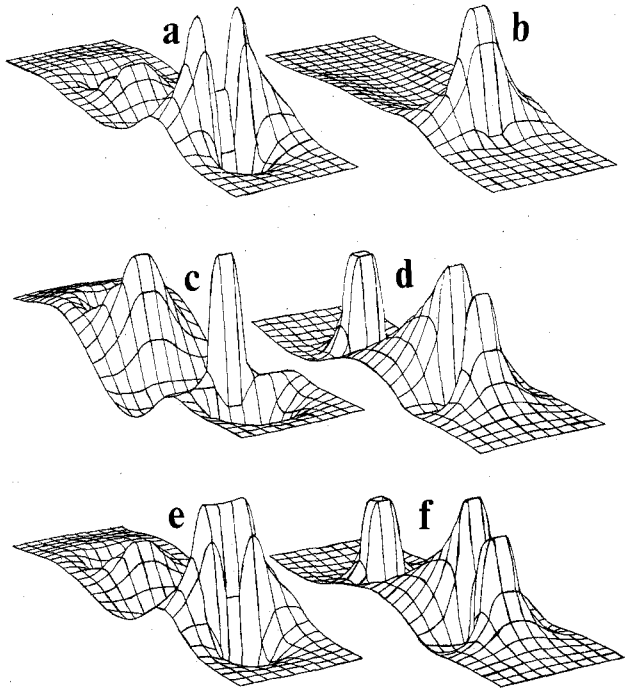

Figure 3. ^{1}H shielding density maps for $x = 0.0625$ au plane of the HF molecule. The density maps shown are for the components (a) σ_{xx}, (b) σ_{zz}, (c) σ_{yy}, (d) $-\sigma_{yy}$, (e) $(\sigma_{xx} + \sigma_{yy} + \sigma_{zz})/3$, and (f) $\sigma_{zz} - (\sigma_{xx} + \sigma_{yy})/2$. Both (c) and (d) are shown to display the features of the density map for σ_{yy} which are above and below the plane (negative shielding density).

nonlinear interpolation to produce relatively smooth contours. Since the density functions can be rapidly changing in some regions of the molecule, the density function has to be specified for a very fine grid of points on the plane in order to get any reasonable contour plots. Another way of displaying a three-dimensional surface is to take a series of parallel traces on the surface, offset from each other by small horizontal (Δz) and vertical (Δy) increments. The vertical and horizontal increments may be chosen to be identical or otherwise. In the figures shown here, the grid of points on the plane were chosen to be equally spaced with the spacing being 0.125 au. The impression of three-dimensionality is enhanced by rotating the plane by some chosen angle ϕ, choosing the view to be some θ degrees above the horizon, and eliminating the "hidden" lines, those sections of a given trace that appear to lie behind a previous trace when viewed from that viewing direction. A perspective view was not chosen in this case, that is, the viewing point was chosen at infinity, so as to avoid any apparent distortion in any inherent symmetry of the density function.

In the examples shown here the shielding density function is calculated as a table of values for a grid of y and z extending beyond the length of the H–F bond. Advantage was taken of the molecular symmetry in obtaining the values of the function for negative y values. Although the figures, as presented, appear to be in terms of the molecular axes, the density function itself is expressed in terms of x, y, and z relative to the center of the nucleus whose shielding is being calculated. A difference between two density functions can then be obtained directly by subtracting corresponding elements of the tables. When the density function is expressed in terms of coordinates relative to the nucleus of interest (as exposed to, with respect to the molecular origin) the large cancelling terms due to that part of the density function which is centered on N will drop out when the density difference map is taken. This is important especially in determining density difference functions such as that due to bond extension, group substitution, change of conformation, hydrogen bonding, or other chemical effects.[6]

Results

The magnetic shielding density maps for components of ^{19}F shielding in the HF molecule are shown in Figure 2.[32] These maps do not differ greatly from the shielding density maps for any spherically symmetric atom or ion except in scale. For example, the density map of the xx component of ^{19}F shielding in HF appears to be not much different from an exponentially damped $(z^2 + y^2)/r^3$ function on the plane x = constant, although there is some indication of the nodal structure that one would expect in a atom which is not described by a 1s wave function. There appears to be very little distortion due to the presence of the H atom in this molecule. The corresponding density maps for ^{19}F shielding in a molecule such as ClF would be considerably different since there would be a substantially larger perturbation in the currents near the F nucleus due to the other atom in ClF than in HF.

The density maps for components of ^{1}H magnetic shielding in HF are shown in Figure 3. This contrasts to the ^{19}F case as follows: (a) These show very definite distortions from the shielding density of a spherically symmetric system. (b) There is a substantial contribution to all components of the ^{1}H shielding from the regions near the other nucleus. (c) Apart from the nonvanishing contributions from regions near the other nucleus, the density maps of the ^{1}H shielding are substantially different in form from that of the ^{19}F shown in Figure 2. Of course, these differences would be considerably smaller for ^{1}H in H_2 molecule. While the density maps of ^{19}F shielding in HF are very similar in form to that of a spherically symmetric atom or ion, those of ^{1}H in HF are quite different. This is clearly shown in Figure 4, where one of the traces on the isotropic σ^H surface for the HF molecule (the trace for $x = 0.0625$ au, $y = 0.0625$ au) is reproduced and compared to the same trace on the diamagnetic shielding surface of the H atom. This comparison indicates to some extent why absolute ^{1}H shieldings are difficult to calculate very accurately. There are cancelling contributions of both signs

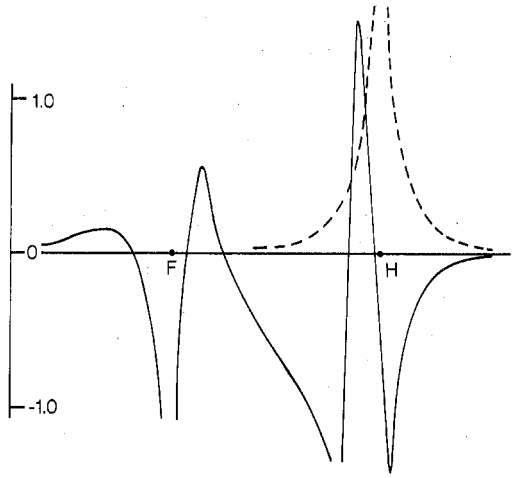

Figure 4. ^{1}H shielding density profiles for HF molecule (solid line) and H atom (broken line). Each shows a trace of the isotropic ^{1}H shielding density, $(\sigma_{xx} + \sigma_{yy} + \sigma_{zz})/3$, for $x = 0.0625$ au, $y = 0.0625$ au.

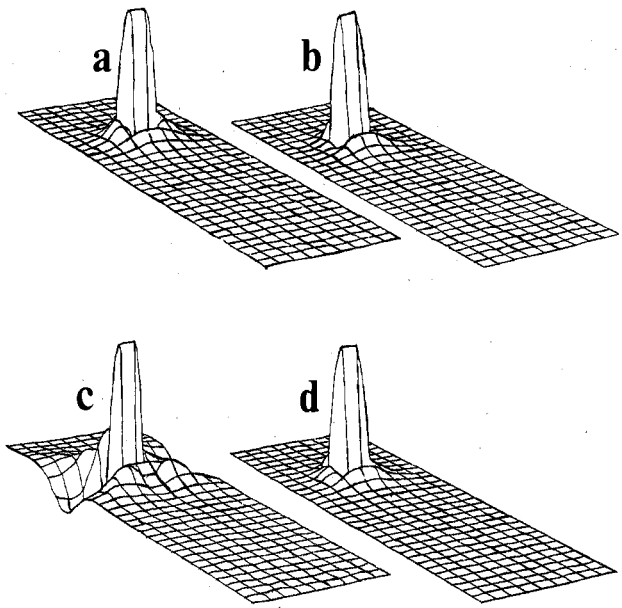

Figure 5. ^{19}F shielding density difference maps for HF molecule minus fluoride ion for the components (a) $-\Delta\sigma_{xx}$, (b) $-\Delta\sigma_{yy}$, (c) $-\Delta\sigma_{zz}$, and (d) $-\Delta(\sigma_{xx} + \sigma_{yy} + \sigma_{zz})/3$.

when the paramagnetic terms are included, whereas the diamagnetic terms can be calculated quite accurately. This has been known for some time and is the basis for the practice of calculating the diamagnetic term by some method and then combining this result with an empirical value of the paramagnetic term obtained from its known relationship with the spin-rotation constant.[33] Indeed it has been found that the diamagnetic terms for both ^{1}H and ^{19}F shielding calculated by multiconfiguration self-consistent field method (MCSCF),[34] which recovers a substantial fraction of electron correlation energy, differs only very slightly from single configuration SCF of even the estimates by Flygare's method.[35]

Charge density differences maps have been found to be very useful in understanding the shifts in electron distribution and polarizations which occur during molecule formation.[3] The magnetic shielding density difference maps are expected to offer some of the same useful physical pictures. The ^{19}F shielding change due to bond formation is obtained by taking the difference between the ^{19}F shielding density in HF and the shielding density in fluoride ion. These difference maps are shown in Figure 5. Basically, we can think of these maps as pictures of

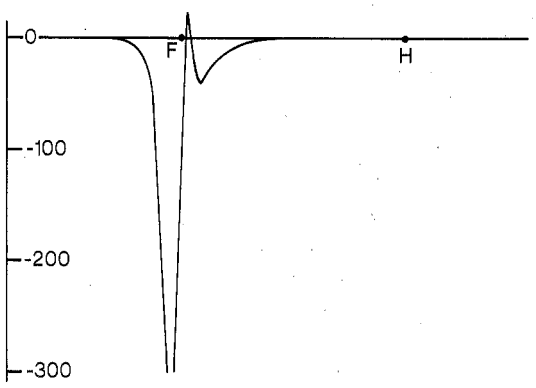

Figure 6. ^{19}F shielding density difference profile for HF molecule minus fluoride ion. This particular trace of the isotropic ^{19}F shielding density difference, $\Delta(\sigma_{xx} + \sigma_{yy} + \sigma_{zz})/3$, is for $x = 0.0625$ au, $y = 0.0625$ au.

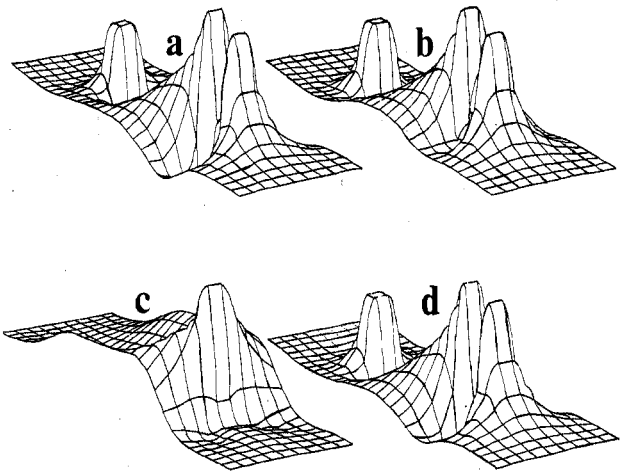

Figure 7. ^{1}H shielding density difference maps for HF molecule minus H atom for the components (a) $-\Delta\sigma_{xx}$, (b) $-\Delta\sigma_{yy}$, (c) $\Delta\sigma_{zz}$, and (d) $-\Delta(\sigma_{xx} + \sigma_{yy} + \sigma_{zz})/3$.

the shielding changes which occur due to the perturbing presence of a bare proton at a distance R from the F^- ion. The bare proton causes polarization of the F^- ion charge distribution,[36] leading to a change in the currents around the F nucleus and, in turn, the currents closest to the nucleus lead to a change in the ^{19}F shielding. When integrated, this density difference function gives the ^{19}F chemical shift between HF and the F^- ion. The difference maps in Figure 5 show a decrease in shielding density due to the polarization of the F^- ion charge by a bare proton. In Figure 6, a trace on the difference map is shown in profile, for the ^{19}F shielding in HF minus fluoride ion. The changes in the current density due to the presence of the bare proton 1.733 au away clearly results in deshielding the ^{19}F nucleus. Most of the deshielding occurs in the immediate vicinity of the ^{19}F nucleus, which would have been expected from the change in charge density profile calculated by Bader et al.[36] and reproduced in Figure 8.

The density difference map for the ^{1}H shielding change due to bond formation is obtained by taking the difference between the ^{1}H shielding density in HF and the diamagnetic shielding density in H atom. These maps are shown in Figure 7 for the various components of σ. Figure 7 shows an increase in ^{1}H shielding density due to the presence of the F atom. This increase is especially marked in the immediate vicinity of the proton although there is some substantial contribution from the far side of the F. The trace in Figure 4 shows a profile of this change. The positive shielding contribution from the far side of the F nucleus probably explains the fair success of the neighbor

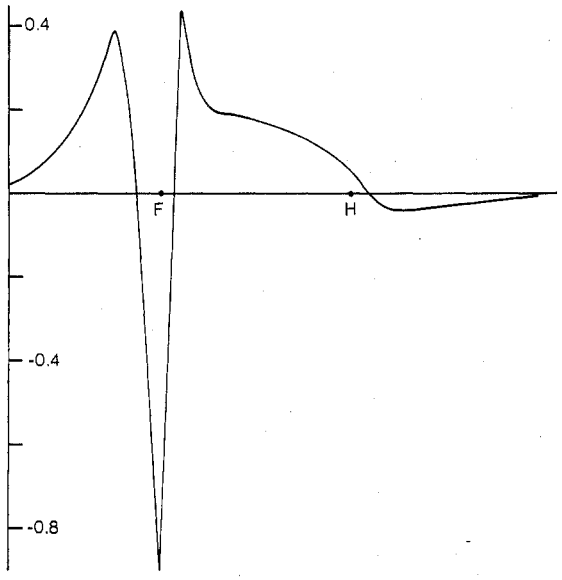

Figure 8. Profile along the internuclear axis of the charge density difference for HF obtained by subtracting the superimposed densities of the undisturbed atoms separated by R_e from the molecular charge density (from Figure 4 of Bader, Keaveny, and Cade, ref 36).

anisotropy model of Pople, which considers the lone pairs on the halogen in estimating the ^1H shifts in HCl, HBr, and HI.[37]

We can see from the profile of charge density change from the calculations of Bader et al.[36] (shown in Figure 8) that the polarizations and charge density shifts which occur upon molecule formation are accompanied by parallel changes in the shielding density profile (see Figure 4). This may be the reason why some correlations of chemical shifts with atomic charge populations calculated by semiempirical or other methods for the ground state of closely related molecules have some degree of success.

Conclusions

We have shown the physical basis for the ^{19}F chemical shift between HF and F^- ion and for the ^1H chemical shift between HF and H atom. Density difference maps showing chemical shifts due to molecule formation may be further investigated by using other small systems so that the shielding or deshielding effects accompanying charge density shifts upon molecule formation may be generalized. This is only the beginning of the general application of shielding density maps. Further work for the immediate future includes the study of hydrogen bonding by showing the shielding density difference maps for both ^1H and ^{19}F in FHF^- compared to HF.[38] The water dimer can also be used as an example. The net ^1H shielding change in H_2O upon dimerization (hydrogen bonding) has been calculated by Ditchfield.[39] The density difference maps for ^1H shielding in the dimer should shed some light on where the chemical shift due to hydrogen bonding is coming from. The effect of a polar solvent molecule may be investigated by considering the system H_2–H_2O at large distances, such that the H_2O molecule appears as an electric dipole from the point of view of the H_2. The difference maps for ^1H shielding in H_2–H_2O minus the isolated H_2 may yield some physical insight into polar solvent effects. The effect of bond extension was investigated previously.[6] The results provide some basis for discussing the derivative of chemical shielding, $(\partial\sigma/\partial R)_{eq}$, which is obtained empirically from temperature-dependent chemical shifts in the gas phase and shifts due to isotopic substitution.[40] An atom or ion in an electric field would suffer some distortion of its charge density. The density difference map for the nucleus in the atom or ion with and without the electric field would provide a physical basis for interpreting the quantities $\sigma^{(1)}_{\alpha\beta\gamma}$ which have been the subject of recent interest,[41,42]

This is a modest beginning of the investigations into the possible utility of shielding density maps. It is expected that these maps will provide a physical basis for discussion of chemical shifts without the necessity of resorting to approximate models to reduce complexity at the expense of sacrificing quantitation.

Acknowledgment. One of the authors (C.J.J.) acknowledges the support of National Science Foundation (CHE 77-09133).

References and Notes

(1) R. F. W. Bader, *MTP Int. Rev. Sci., Phys. Chem., Ser. Two*, **1**, 43 (1975).
(2) R. F. W. Bader and W. H. Henneker, *J. Am. Chem. Soc.*, **87**, 3063 (1965).
(3) R. F. W. Bader, W. H. Henneker, and P. E. Cade, *J. Chem. Phys.*, **46**, 3341 (1967).
(4) R. F. W. Bader and A. D. Bandrauk, *J. Chem. Phys.*, **49**, 1666 (1968).
(5) A. Streitwieser, Jr., and P. H. Owens, "Orbital and Electron Density Diagrams", Macmillan, New York, 1973.
(6) C. J. Jameson and A. D. Buckingham, to be published.
(7) D. W. Jones in "Nuclear Magnetic Resonance", Vol. 7, R. K. Harris, Ed., The Chemical Society, London, 1978.
(8) E. Schrodinger, *Ann. Phys.*, **81**, 137 (1927); **82**, 265 (1927).
(9) C. P. Slichter, "Principles of Magnetic Resonance", Springer-Verlag, Berlin, 1978.
(10) W. N. Lipscomb, *MTP Int. Rev. Sci., Phys. Chem., Ser. One*, **1**, 167 (1972).
(11) R. Ditchfield, *Chem. Phys. Lett.*, **40**, 53 (1976).
(12) B. Day and A. D. Buckingham, *Mol. Phys.*, **32**, 343 (1976).
(13) P. Swanstrom, W. P. Kraemer, and G. H. F. Diercksen, *Theor. Chim. Acta*, **44**, 109 (1977).
(14) M. Zaucer, D. Pumpernik, M. Hladnik, and A. Azman, *Z. Naturforsch. A*, **32**, 411 (1977).
(15) A. J. Sadlej, *Chem. Phys. Lett.*, **36**, 129 (1975); **30**, 432 (1975).
(16) R. McWeeny, *Phys. Rev.*, **126**, 1028 (1962).
(17) G. H. F. Diercksen and R. McWeeny, *J. Chem. Phys.*, **44**, 3554 (1966).
(18) W. N. Lipscomb, *Adv. Magn. Reson.*, **2**, 137 (1966).
(19) A. Dalgarno, *Proc. R. Soc. London, Ser. A*, **232**, 267 (1959).
(20) M. Karplus and H. J. Kolker, *J. Chem. Phys.*, **38**, 1263 (1963).
(21) J. M. Schulman and J. I. Musher, *J. Chem. Phys.*, **49**, 4845 (1968).
(22) D. E. O'Reilly, *J. Chem. Phys.*, **36**, 855 (1962).
(23) E. Ishiguro and S. Koide, *Phys. Rev.*, **94**, 350 (1954).
(24) T. K. Rebane, *Opt. Spectrosc.*, **8**, 242 (1960).
(25) T. Caves and M. Karplus, *J. Chem. Phys.*, **50**, 3649 (1969).
(26) R. M. Stevens, R. M. Pitzer, and W. N. Lipscomb, *J. Chem. Phys.*, **38**, 550 (1963).
(27) R. Ditchfield, *J. Chem. Phys.*, **56**, 5688 (1972).
(28) S. T. Epstein, *J. Chem. Phys.*, **58**, 1592 (1973).
(29) G. C. Lie and E. Clementi, *J. Chem. Phys.*, **60**, 1275 (1974).
(30) J. L. Dodds, R. McWeeny, W. T. Raynes, and J. P. Riley, *Mol. Phys.*, **33**, 611 (1977).
(31) The calculations were carried out at Cambridge University with the ATMOL3 package of programs from the Atlas Computer Laboratory.
(32) It should be pointed out that these maps are not the same as the isoshielding contour maps such as have been used to show the ring currents contributions or other neighbor contributions to σ at various locations in space. Note also that these maps represent the shielding density function in one plane and are not meant to be pictures of the entire density function.
(33) W. H. Flygare, *Chem. Rev.*, **74**, 653 (1974).
(34) R. D. Amos, *Mol. Phys.*, **35**, 1765 (1978).
(35) T. D. Gierke and W. H. Flygare, *J. Am. Chem. Soc.*, **94**, 7277 (1972).
(36) R. F. W. Bader, I. Keaveny, and P. E. Cade, *J. Chem. Phys.*, **47**, 3381 (1967).
(37) J. A. Pople, *Proc. R. Soc. London, Ser. A*, **239**, 541, 550 (1957).
(38) See ref 11, 14, and 15.
(39) R. Ditchfield, *J. Chem. Phys.*, **65**, 3123 (1976).
(40) See review by W. T. Raynes in "Nuclear Magnetic Resonance", Vol. 8, R. K. Harris, Ed., The Chemical Society, London, 1978.
(41) A. J. Sadlej and W. T. Raynes, *Mol. Phys.*, **35**, 101 (1978).
(42) J. P. Riley and W. T. Raynes, *Mol. Phys.*, **32**, 569 (1976).